

See discussions, stats, and author profiles for this publication at: <https://www.researchgate.net/publication/10678177>

# Delta-wing function of webbed feet gives hydrodynamic lift for swimming propulsion in birds

Article in *Nature* · August 2003

DOI: 10.1038/nature01695 · Source: PubMed

---

CITATIONS

84

---

READS

705

2 authors:



[L. Christoffer Johansson](#)

Lund University

63 PUBLICATIONS 2,357 CITATIONS

[SEE PROFILE](#)



[Rolf Åke Norberg](#)

University of Gothenburg

39 PUBLICATIONS 2,636 CITATIONS

[SEE PROFILE](#)

3 July 2003

International weekly journal of science

# nature

£4.95

[www.nature.com/nature](http://www.nature.com/nature)

## Delta force

Fluid dynamics of  
delta-shaped hydrofoils  
in animals

**Mammalian pheromones** Maternal guidance

**Mathematics** Computer-aided proof adds up to trouble

**Ultracold matter** Bosons from fermions

**naturejobs** adjunct professors stay in touch





3 July 2003

## Delta force: Fluid dynamics of delta-shaped hydrofoils in animals

Cover image: Björn Norberg ([www.bnillustrations.com](http://www.bnillustrations.com))

Delta-shaped hydrofoils and aerofoils have originated repeatedly and independently in nature in a wide variety of animals, so they must be effective. The function of a delta used for propulsion in water is shown by studies of videos of a diving great cormorant and a model foot made of sheet aluminium. The computer-generated image on the cover shows a bird's webbed foot in the later phase of the power stroke, its upper side facing down, as the bird exits to the right. The foot is operating in lift mode, generating the vortex system characteristic of an inverted delta wing. Propulsive forces are produced throughout the power stroke, first from drag, later from lift.

### Delta-wing function of webbed feet gives hydrodynamic lift for swimming propulsion in birds

L. CHRISTOFFER JOHANSSON & R. ÅKE NORBERG  
*Nature* **424**, 65–68 (2003); doi:10.1038/nature01695

## Delta-wing function of webbed feet gives hydrodynamic lift for swimming propulsion in birds

L. Christoffer Johansson\* & R. Åke Norberg†

\* Department of Organismic and Evolutionary Biology, Harvard University, 26 Oxford Street, Cambridge, Massachusetts 02138, USA

† Department of Zoology, Göteborg University, Box 463, SE-405 30 Göteborg, Sweden

Most foot-propelled swimming birds sweep their webbed feet backwards in a curved path that lies in a plane aligned with the swimming direction. When the foot passes the most outward position, near the beginning of the power stroke, a tangent to the foot trajectory is parallel with the line of swimming and the foot web is perpendicular to it. But later in the stroke the foot takes an increasingly transverse direction, swinging towards the longitudinal axis of the body. Here we show that, early in the power stroke, propulsion is achieved mostly by hydrodynamic drag on the foot, whereas there is a gradual transition into lift-based propulsion later in the stroke. At the shift to lift mode, the attached vortices of the drag-based phase turn into a starting vortex, shed at the trailing edge, and into spiralling leading-edge vortices along the sides of the foot. Because of their delta shape, webbed feet can generate propulsive forces continuously through two successive modes, from drag at the beginning of the stroke, all the way through the transition to predominantly lift later in the stroke.

Foot propulsion in swimming birds has generally been considered to be drag-based, both in surface swimming and during diving<sup>1,2</sup>. Drag is the hydrodynamic force that opposes movement



through a fluid; it is aligned with the movement but acts in the opposite direction. This mode requires that the foot is moved backwards in a still-water frame of reference. The foot must therefore move backwards faster, relative to the bird, than it swims. An entirely different mode of foot-propelled swimming has recently been detected in the great crested grebe (*Podiceps cristatus*)<sup>3,4</sup>. It does not paddle with its feet in a fore-and-aft movement, but instead sweeps its feet outwards-upwards in a transverse plane, perpendicular to the swimming direction. There is no backward movement of the feet relative to the water, so drag cannot be tilted forwards and so is useless for propulsion. Instead, propulsion is based on lift, which here is directed forwards and is nearly perpendicular to the path of the foot<sup>3,4</sup>, being by definition normal to the resultant relative flow. There are two functional benefits from using lift rather than pure drag for propulsion. First, with drag-based propulsion, muscle work is done directly against the entire reaction force on the foot, whereas work is done against only a component of it when propulsion is based on lift. And that component is often smaller than the propulsive force. In lift mode it is therefore possible to exploit a propulsive force that is larger than the force against which work is being done. This enhances hydrodynamic efficiency and energy economy. Second, with drag-based propulsion the feet must move backwards in still water, so the bird must sweep its feet faster than it swims. With lift-based propulsion it need not do so, which again improves energy economy and also might allow higher swimming speeds because the sweep velocity of the foot in lift mode need not be nearly as high as the swimming speed.

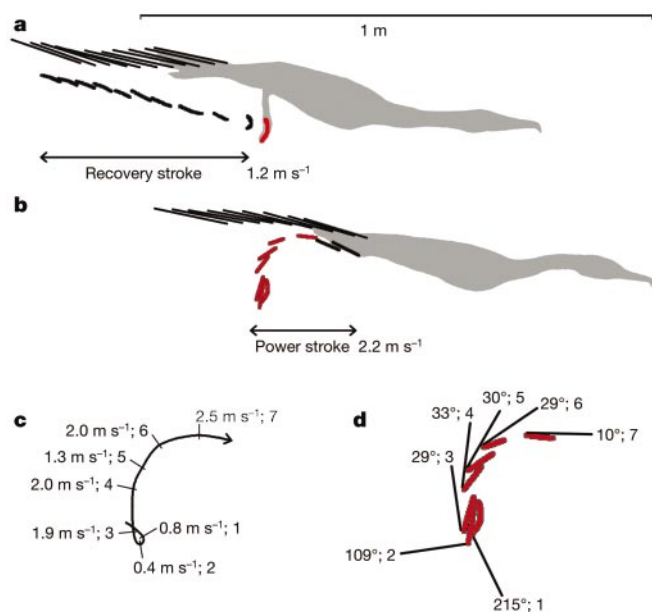


**Figure 1** Tracings from a video sequence (separated by 0.02 s) of a foot-stroke cycle of a diving cormorant. Bold lines indicate the position and orientation of the foot, and thin lines show the dorsal side of the tail. **a**, The recovery stroke with the shaded bird at the start of the power stroke. **b**, The power stroke, starting with the same foot position that terminated the upper sequence. The shaded bird is at the end of the power stroke. Acceleration of the body occurs over seven video fields (from 1.2 m s<sup>-1</sup> at the end of recovery stroke to 2.2 m s<sup>-1</sup> at position 7 of the power stroke), indicated by the red foot. **c**, **d**, Data for the acceleration phase of **b**. **c**, The instantaneous still-water speed of the trailing edge of the foot is indicated at positions 1–7 along its trajectory. **d**, The instantaneous angle of attack at the trailing edge of the foot is indicated at the same seven foot positions. The drag mode can last, at most, for as long as the foot moves backwards relative to the still water, which it does until slightly after position 3, during which time the angle of attack changes from ~215° to less than 30°. This is 39% of the duration of the power stroke. During the remainder of the power stroke, 61% of the time, the body continues to accelerate forwards, owing entirely to lift.

Here we show that the more conventional fore-and-aft movement of the feet in swimming birds can also generate thrust that is based on hydrodynamic lift. Our results are based on observations and analyses of video films of swimming and diving birds (Fig. 1), and on flow-visualization experiments with a model foot in a simulated power stroke (Fig. 2).

We distinguish three phases of the power stroke. Phase 1 is when the foot performs a largely translatable backward movement near the start of the power stroke. A recirculating wake is formed on the leeward, suction side of the foot, and a closed vortex, surrounding the foot, is rolled up behind its edges. At this stage, the foot moves backwards relative to the water and water meets the foot at nearly right angles to its web. Water is accelerated and drawn backwards along with the foot, over its leeward surface, and the induced flow is bounded by an attached closed vortex. The reaction force on the foot is hydrodynamic drag, directed forwards, opposite to the direction of movement of the foot. It is the useful propulsive force at this stage (Fig. 3).

Because of rotation of the leg, the outer, distal edge of the foot moves faster than its proximal parts, and this velocity gradient creates a stronger suction at the distal edge and a lower pressure within the vortex core there. Water should therefore be drawn towards the foot's trailing edge on the suction side and spiral rearwards in the side-edge vortices, similar to the spanwise, leading-edge flow over flapping insect wings<sup>5</sup>. In this way a rearward flow is set up on the suction side, typical for a wing in lift mode.

Stage 2 of the power stroke occurs after the foot has passed its most outward position: the path curves inwards, towards the longitudinal body axis of the bird. The transverse speed component therefore increases gradually while the backward speed component diminishes. The backward speed component very soon becomes lower than the bird's swimming speed, so the foot no longer moves backwards relative to the water but instead moves forwards with the bird. When this happens, the drag force cannot be tilted forwards, so propulsion is no longer drag-based (Figs 1 and 3).

When the foot starts moving transversely in relation to the swimming direction, it leaves behind the previous, attached, trailing-edge vortex, which now becomes a starting vortex for a drawn-out, U-shaped vortex behind the foot. The vortices that were attached to the sides of the foot in drag mode turn into spiralling leading-edge vortices, which leave stable, trailing tip-vortices behind the outer corners of the foot, as on delta-wings<sup>6,7</sup>. They form the sides of the shed U-shaped vortex (Figs 2 and 3).

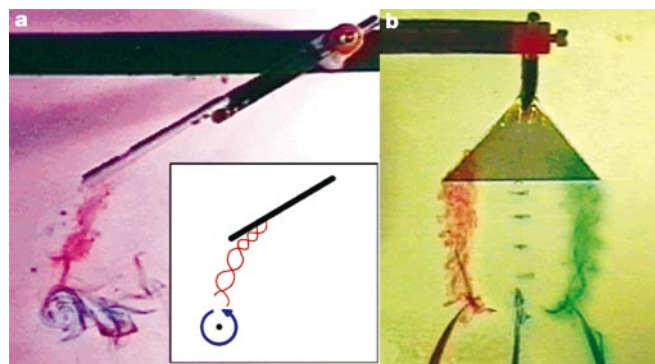


**Figure 2** Side and front views of the model foot simulating a power stroke of a swimming bird. **a**, Side view. The foot rotates in a clockwise direction and also translates to the right. **b**, Front view, showing the leeward, suction, side of the foot as seen from the right side in **a**. The flow swirls around the swept-back side edges of the model foot, over to its suction side, where it is entrained in an attached leading-edge vortex that is subsequently shed from the outer corner of the foot to form a spiralling, trailing tip-vortex. The side view also shows a transverse starting vortex left behind in the wake when the model foot moves upwards and to the right.

Circulation is in the same sense as when the vortices were attached to the foot when it translated backwards, in drag mode. Enclosed by the U-shaped vortex is a jet of water flowing backwards at about right angles to the vortex plane. In addition the vortex itself is convected downstream, but at a slower speed than the induced jet (Fig. 3).

Lift production should be facilitated early in the lift phase because there is probably a rearward flow along the suction side of the foot already in drag mode. In addition, the trailing-edge vortex—also developed in drag mode—is just shed as a starting vortex at the transition to lift mode, and the attached side-edge vortices are also built up in drag mode and later turn directly into leading-edge vortices in the lift phase.

When the relative water velocity due to the swimming speed is added vectorially to the velocity due to the foot movement relative to the bird, tangential to the stroke path, the resultant relative water speed is seen to meet the foot from obliquely in front, forming an acute angle of attack with the foot (Fig. 3). This angle depends on the position of the foot in its path and on the relation between the swimming speed and the stroke speed, variables that change throughout the power stroke and along the foot.

The reaction force on the foot is directed obliquely forwards, and is opposite to the direction of the water flow in the jet enclosed by

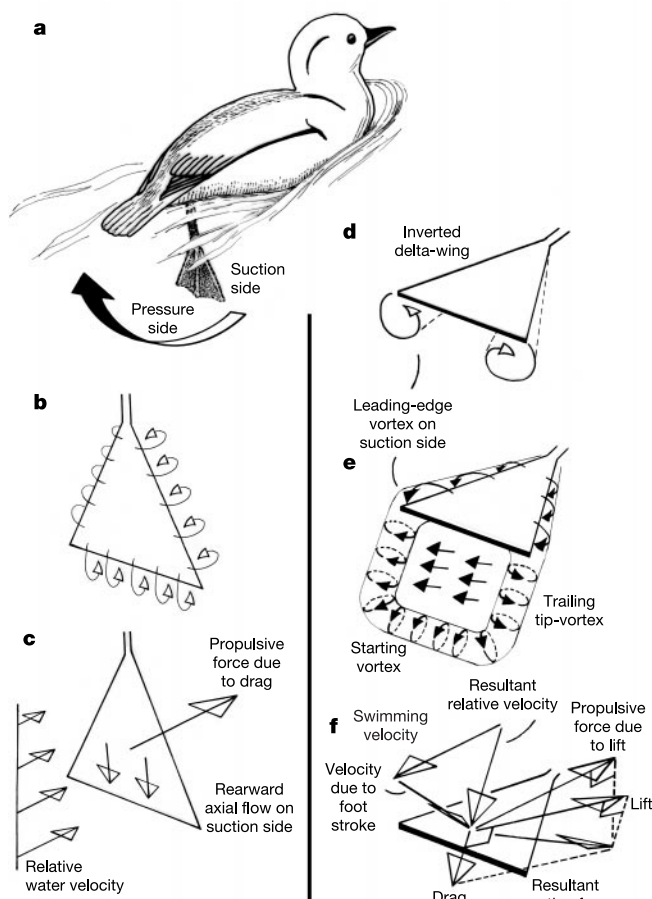


**Figure 3** Schematic, generalized representation of flow patterns and forces set up by a webbed foot during a power stroke of a bird in fast swimming. **a**, Definition of suction side and pressure side of the foot in backward motion. The elicited forces are inferred from the induced water flow, as observed in our flow-visualization experiments. **b**, **c**, The foot in drag mode; **d**–**f**, the foot in lift mode at a later stage of the power stroke. The ratio of swimming velocity to foot-stroke velocity used for **f** is roughly as in lift mode at foot position 6 in Fig. 1, and the lift-to-drag ratio is just an example for one phase of the stroke. All velocity and force vectors lie in a common plane aligned with the line of swimming.

the vortex. It is only because of the production of a lift force that the resultant reaction force gets a forward inclination, owing to which there is a forward force vector. This is the useful propulsive force and it is due entirely to lift. Drag forces on the foot only detract from the propulsive force at this stage (Fig. 3).

In phase 3, at the end of the power stroke the foot is furled and pulled out of the wake and the U-shaped vortex closes after the foot to form an ellipse.

The motion of the model foot in this study is the simple consequence of adding a rotary, sweeping, motion of the foot to the forward velocity of the bird. This suggests that the mechanism described here might also be exploited by other swimming animals with webbed feet or fins. The  $\Delta$  form occurs in the caudal fins of arrow-worms (phylum Chaetognatha), the caudal and pectoral fins of fishes, in the webbed feet of frogs and most swimming birds, the hind flippers of seals, and the tail flukes of whales and dugongs. In addition, the tail of many birds attains a perfect  $\Delta$  form when activated and spread, owing to its  $\Delta$ -notched form when furled. Its delta-wing function has recently been treated theoretically<sup>8</sup> and verified on swallow tails<sup>9</sup>. Hydrofoils and airfoils with a  $\Delta$  form have thus originated repeatedly and independently by striking evolutionary convergence among widely separate phyletic lines.

A characteristic of a delta-wing is that it is almost un stallable and continues to give large lift forces even at very large angles of attack, although at the penalty of high drag<sup>6,7</sup>. The fluid dynamics of the  $\Delta$  form is also insensitive to differences in size and speed, as reflected in the Reynolds number<sup>7</sup>. These features enable a  $\Delta$ -shaped foot or fin to produce large propulsive forces during the entire power stroke when it operates in two successive modes, from pure drag in the beginning of the stroke, all the way through the transition to predominantly lift in later stages. □

## Methods

The kinematics of a diving great cormorant (*Phalacrocorax carbo*) was determined by an analysis of video sequences resolved into 50 fields  $s^{-1}$ . The velocities of the bird and the feet were estimated by applying a cubic spline fit<sup>10</sup> to the kinematic data. Angles of attack at the distal end of the feet were determined as the angle between the instantaneous, local velocity vector and the foot as seen in lateral view (Fig. 1).

We swept a model foot through water in a movement pattern closely mimicking the natural movement of the diving cormorant. The foot was made of a 2-mm-thick sheet of aluminium, had an isosceles triangular planform with lateral sides 100 mm long, a distal side 85 mm long and a sweepback angle of 65°. This is a simplified, generalized planform for the model foot that is meant to represent the webbed feet of most swimming birds (even though the cormorant foot has a skewed, triangular planform). The paddling movement of the foot was achieved by using a device consisting of two wheels (250 mm diameter) mounted 150 mm apart on a common horizontal axis, which extended 200 mm on the outer side of one of the wheels. The axis was fixed so that it rotated with the wheels. A thin bar was fastened at 90° to the sticking-out free end of the axis, like a single spoke, and the model foot was attached with its leading apex to the distal end of this transverse bar. The entire device was placed on a horizontal ramp inside a water tank. Ramp elevation was adjusted so that the foot became submerged to a suitable depth in water. By adjusting the length of the transverse bar in relation to the radius of the wheels, it was possible to mimic the natural foot movement in a power stroke. The wheels were rolled manually on the ramp as required to simulate a power stroke. The forward movement of the wheel axis corresponded to the bird's swimming speed, and rotation of the axis with the attached model simulated the foot sweep. This combination of a transitory, forward motion of the body and a rotary, backward sweep of the foot characterizes the kinematics of most swimming birds that use a backward power stroke confined to a plane aligned with the line of swimming. We revealed the induced water flow with a dye ejected via plastic tubes with an internal diameter of 1.14 mm; the tubes were attached along the oblique leading edge on the pressure side of the model foot. The flow thus revealed was examined on video films (Fig. 2).

Received 23 December 2002; accepted 22 April 2003; doi:10.1038/nature01695.

- Blake, R. W. Mechanics of drag-based mechanisms of propulsion in aquatic vertebrates. *Symp. Zool. Soc. Lond.* **48**, 29–52 (1981).
- Braun, J. & Reif, W.-E. A survey of aquatic locomotion in fishes and tetrapods. *N. Jb. Geol. Paläont. Abh.* **169**, 307–332 (1985).
- Johansson, L. C. & Lindhe Norberg, U. M. Asymmetric toes aid underwater swimming. *Nature* **407**, 582–583 (2000).
- Johansson, L. C. & Lindhe Norberg, U. M. Lift-based paddling in diving grebe. *J. Exp. Biol.* **204**, 1687–1696 (2001).
- Ellington, C. P., van den Berg, C., Willmott, A. P. & Thomas, A. L. R. Leading-edge vortices in insect flight. *Nature* **384**, 626–630 (1996).
- Katz, J. & Plotkin, A. *Low-speed Aerodynamics* (McGraw-Hill, New York, 1991).

7. Lee, M. & Ho, C.-M. Lift force of delta wings. *Appl. Mech. Rev.* **43**, 209–221 (1990).
8. Thomas, A. L. R. On the aerodynamics of birds' tails. *Phil. Trans. R. Soc. Lond. B* **340**, 361–380 (1993).
9. Norberg, R. Å. Swallow tail streamer is a mechanical device for self-deflection of tail leading edge, enhancing aerodynamic efficiency and flight manoeuvrability. *Proc. R. Soc. Lond. B* **257**, 227–233 (1994).
10. Walker, J. A. QuickSAND. Quick Smoothing and Numerical Differentiation for the Power Macintosh (<http://www.usm.maine.edu/~walker/software.html>) (1997).

**Acknowledgements** We thank B. Svensson for building the mechanical experimental device.

**Competing interests statement** The authors declare that they have no competing financial interests.

**Correspondence** and requests for materials should be addressed to R.Å.N. (ake.norberg@zool.gu.se).